J Neurophysiol 89: 290–303, 2003;
10.1152/jn.00160.2001.

Coordinated Turn-and-Reach Movements. II. Planning in an External Frame of Reference

PASCALE PIGEON, SIMONE B. BORTOLAMI, PAUL DIZIO, AND JAMES R. LACKNER
Ashton Graybiel Spatial Orientation Laboratory, Brandeis University, Waltham, Massachusetts 02454-9110

Submitted 26 February 2001; accepted in final form 6 September 2002

Pigeon, Pascale, Simone B. Bortolami, Paul DiZio, and James R. Lackner. Coordinated turn-and-reach movements. II. Planning in an external frame of reference. *J Neurophysiol* 89: 290–303, 2003; 10.1152/jn.00160.2001. The preceding study demonstrated that normal subjects compensate for the additional interaction torques generated when a reaching movement is made during voluntary trunk rotation. The present paper assesses the influence of trunk rotation on finger trajectories and on interjoint coordination and determines whether simultaneous turn-and-reach movements are most simply described relative to a trunk-based or an external reference frame. Subjects reached to targets requiring different extents of arm joint and trunk rotation at a natural pace and quickly in normal lighting and in total darkness. We first examined whether the larger interaction torques generated during rapid turn-and-reach movements perturb finger trajectories and interjoint coordination and whether visual feedback plays a role in compensating for these torques. These issues were addressed using generalized Procrustes analysis (GPA), which attempts to overlap a group of configurations (e.g., joint trajectories) through translations and rotations in multi-dimensional space. We first used GPA to identify the mean intrinsic patterns of finger and joint trajectories (i.e., their average shape irrespective of location and orientation variability in the external and joint workspaces) from turn-and-reach movements performed in each experimental condition and then calculated their curvatures. We then quantified the discrepancy between each finger or joint trajectory and the intrinsic pattern both after GPA was applied individually to trajectories from a pair of experimental conditions and after GPA was applied to the same trajectories pooled together. For several subjects, joint trajectories but not finger trajectories were more curved in fast than slow movements. The curvature of both joint and finger trajectories of turn-and-reach movements was relatively unaffected by the vision conditions. Pooling across speed conditions significantly increased the discrepancy between joint but not finger trajectories for most subjects, indicating that subjects used different patterns of interjoint coordination in slow and fast movements while nevertheless preserving the shape of their finger trajectory. Higher movement speeds did not disrupt the arm joint rotations despite the larger interaction torques generated. Rather, subjects used the redundant degrees of freedom of the arm/trunk system to achieve similar finger trajectories with differing joint configurations. We examined finger movement patterns and velocity profiles to determine the frame of reference in which turn-and-reach movements could be most simply described. Finger trajectories of turn-and-reach movements had much larger curvatures and their velocity profiles were less smooth and less bell-like in trunk-based coordinates than in external coordinates. Taken together, these results support the conclusion that turn-and-reach movements are controlled in an external frame of reference.

INTRODUCTION

Turning and reaching movements can generate substantial Coriolis, centripetal, and inertial interaction torques because of the motion of the arm relative to the rotating trunk. Nevertheless, as shown in the companion paper, reaching accuracy is little if at all affected although high arm-projection and trunk-rotation velocities are being generated simultaneously. The present paper assesses what influence self-generated interaction torques have on movement trajectories considered in terms of joint trajectory patterns and external space coordinates. This assessment involves primarily the use of generalized Procrustes analysis, an approach introduced to the study of arm movements by Haggard and his colleagues (Haggard and Richardson 1996; Haggard et al. 1995). It allows one to rearrange trajectories across the workspace and to identify the relative intrinsic variability (the variability in shape of the trajectories) versus extrinsic variability (the variability in location and orientation of the trajectories within the workspace) of the patterns. In particular, this analysis allowed us to investigate whether the intrinsic shape of joint and hand space trajectories remains invariant across speed and vision conditions during turning and reaching movements. We also analyzed whether the neurophysiological implementation of the movement trajectories would be simplified by being represented in intrinsic (i.e., trunk relative) or extrinsic coordinates. This was achieved by examining the position and velocity patterns of the movements in the different reference frames. In an upcoming paper, we will treat quantitatively the movement dynamics of the movement trajectories presented here and describe the actual joint torques associated with the movements (for some preliminary results, see Bortolami et al. 1999).

METHODS

Subjects

Seven individuals (5 male, 2 female) participated. They ranged in age from 19 to 55 yr and were without physical or neurological disorders that would have impaired their performance on the experimental task. They signed an informed consent form approved by the Brandeis Human Subjects Committee.

Apparatus and procedure

Full details are presented in the preceding paper. In brief, subjects stood in front of a high table with a semicircular cut out. Three

Address for reprint requests: P. Pigeon, Ashton Graybiel Spatial Orientation Laboratory, MS 033, Brandeis University, P.O. Box 549110, Waltham, MA 02454-9110 (E-mail: pigeon@brandeis.edu).

The costs of publication of this article were defrayed in part by the payment of page charges. The article must therefore be hereby marked "*advertisement*" in accordance with 18 U.S.C. Section 1734 solely to indicate this fact.

light-emitting diodes (LEDs) embedded in the table surface but not localizable by touch served as targets. An LED would be illuminated when the subject depressed a microswitch located at the body midline near the edge of the table. The LED was extinguished when the microswitch was released at the onset of a trial. The targets were positioned such that one (T1) required substantial leftward trunk rotation and arm projection, one (T2) involved comparable arm projection without significant trunk rotation, and one (T3) substantial trunk rotation (although less than to T1) but without arm projection.

There were four experimental conditions, each including nine movements to each of the three targets, which involved two speeds (slow/fast) and two illumination (light/dark) levels: LS, LF, DS, DF. The room lights were on in the light conditions and off in the dark conditions in which the subjects would reach to the remembered position of the just extinguished target. The slow movements were at a pace to pick up a utensil on a table, the fast to trap an agile insect. The order of the 108 individual trials (4 conditions $\times$ 3 targets $\times$ 9 repetitions) across the four conditions was randomized for each subject.

Data recording and analysis

An OPTOTRAK motion analysis system was used to record (200 Hz) infrared emitters attached to the body to permit resolution of head, trunk, arm, and hand positions in space and shoulder, elbow, and wrist angles. The latter turned out not to be a significant factor because subjects did not change their wrist angles appreciably within or between trials. Consequently, it is not included in the results or analysis.

Computer algorithms were used to calculate finger trajectory, coordination of trunk and hand and arm movements, interjoint coordination, and reaching accuracy. Further details of recording and analysis were presented in the preceding paper.

INFLUENCE OF INTERACTION TORQUES ON FINGER TRAJECTORY AND INTERJOINT COORDINATION. As the velocity of movements involving turning and reaching increases, so does the magnitude of interaction torques—including Coriolis torques—that act on the arm as it extends away from the rotating trunk. In the preceding paper, a simplified dynamic model of the arm/trunk system revealed that the interaction torques contingent on trunk motion acted to extend the arm joints over most of the movements. We tested the hypothesis that the larger interaction torques generated during rapid reaching movements may affect the intrinsic patterns of the finger trajectory and interjoint coordination. For example, larger Coriolis, centripetal, and inertial torques induced by rapid trunk rotation may modify the trajectory of the hand to T1 and impede or delay shoulder flexion if they are not appropriately compensated by muscle torques in the arm joints. In addition, we tested the hypothesis that visual feedback plays a role in the compensation of interaction torques.

To define the interjoint coordination of the reaching movements, vectors joining the wrist, elbow, and right and left shoulders were determined using the coordinates in the horizontal plane of appropriate LED markers. The elbow and shoulder angles were computed based on the dot products of these vectors. The trunk rotation angle was defined in the horizontal plane as the angle between the line joining the right and left shoulder markers and the frontal plane identified by the *yz* axes of the table coordinate system (cf. Fig. 1 in preceding paper). Movements of the wrist joint were minor and neglected (mean wrist excursion across conditions and targets: $<7°$). Leftward trunk rotation, shoulder, and elbow flexion were considered positive, with 0° indicating a trunk parallel to the frontal plane, an upper arm colinear with both shoulders and a fully extended elbow.

To investigate the intrinsic patterns of finger trajectory and interjoint coordination across movement speed and visual feedback conditions, we used generalized Procrustes analysis (GPA). This method has been explained in mathematical detail by Gower (1975) and has been applied to the analysis of hand and joint paths by Haggard et al. (1995) and Haggard and Richardson (1996). GPA calculates the mean of a group of configurations (e.g., joint trajectories) by attempting to translate and rotate the corresponding points of each configuration onto each other configuration, using an iterative least-squares procedure. The mean of the transformed configurations is called the *consensus* configuration, and the variability in shape of the configurations about the consensus represents their *intrinsic* variability. GPA thus distinguishes between the variability in shape of several configurations and the variability in their location and orientation within the workspace. The latter is called *extrinsic* variability and is removed by performing GPA.

Two-dimensional external space trajectories (finger position in the horizontal plane) and three-dimensional joint space trajectories (trunk, shoulder, and elbow angles) of reaching movements from the start position to each target were submitted to GPA. To perform the analysis, each set of nine finger or joint trajectories to the same target performed by a subject in each of the four experimental conditions (LS, LF, DS, DF) had to involve the same number of data points. After calculating that the mean length of the finger trajectory in reaching movements to T1–T3 was ~60, 31, and 37 cm, respectively, each movement was spatially resampled by taking 61, 32, or 38 positions of the finger spaced at ~1-cm intervals. For consistency, the joint trajectories were also resampled such that each would be accordingly composed of 61, 32, or 38 equally spaced data points in joint space.

Because the reaching movements were not constrained except by the experimental table, both finger and joint trajectories exhibited trial-to-trial variation in shape (intrinsic variability) as well as location and orientation (extrinsic variability) in the workspace. For joint trajectories, the intrinsic variability was due in part to the kinematic redundancy of the human arm/trunk system in these movements, such that to produce a given finger trajectory to a target, the CNS could select among an infinite number of patterns of interjoint coordination. Joint redundancy was also partly responsible for the extrinsic variability of joint trajectories because it allowed joint trajectories that were similar in shape but located in different portions of joint space to produce similar finger trajectories.

Two methods were used to test whether the intrinsic patterns of finger and joint trajectories to each target changed across speed and vision conditions (Haggard and Richardson 1996; Haggard et al. 1995). The first method was based on the curvature of the consensus configuration, taken as the mean absolute distance of each of the 61, 32, or 38 datapoints in the consensus configuration from the first principal axis for movements to T1–T3, respectively. The principal axes of the consensus configuration were found using principal component (PC) analysis (Johnson and Wichern 1992), a statistical method that reduces the relationship between n variables (e.g., the elbow, shoulder, and trunk rotation angles) to n linear combinations between them (the principal components). The first of the n orthogonal principal axes is aligned with the direction of maximal data elongation in multidimensional space (Fig. 1*D*). For each subject and target, the curvature of the consensus configuration derived from finger or joint trajectory data was measured for the four experimental conditions. ANOVAs of the curvature measure across speed and vision conditions were performed separately for each subject.

The second method used to investigate the intrinsic patterns of finger and joint trajectories to the three targets relied on root-mean-square (rms) residuals calculated following GPA. The residual quantified how deviant the intrinsic pattern of a particular trajectory was relative to that of the consensus: the more dissimilar the trajectory, the larger its residual. The rms residual of each transformed finger trajectory was calculated by summing the squared distances of each datapoint in the trajectory to the corresponding datapoint in the consensus configuration, averaging the total over the number of datapoints (61, 32, or 38, depending on the target), and calculating the square root. For each subject, the residual of each finger trajectory was

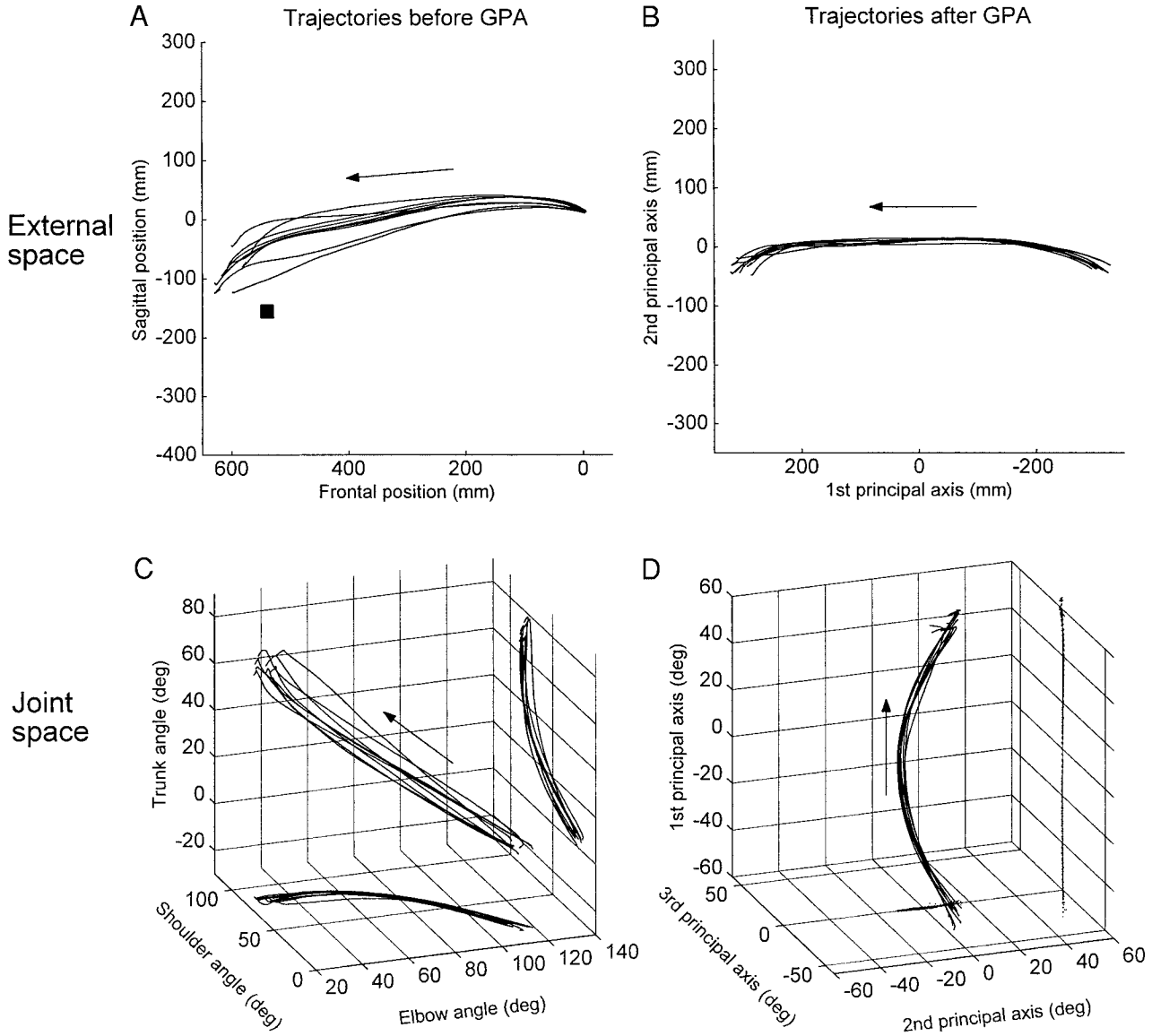

FIG. 1. Finger (*top*) and joint (*bottom*) trajectories of the nine reaching movements to T1 performed by *subject S1* in the dark-fast (DF) condition before (*left*) and after (*right*) generalized Procrustes analysis (GPA). ■, the position of the target. The transformed trajectories in *B* and *D* are shown relative to the principal axes of the consensus configurations. For clarity, 2 plane projections are shown for the joint trajectories before and after transformation.

calculated after GPA was applied to each set of nine movements to the same target performed in the same experimental condition (e.g., LS). In addition, the residual of each finger trajectory was calculated after GPA was applied to sets of 18 movements to the same target pooled together from a pair of experimental conditions (e.g., LS and LF). With four different experimental conditions, six different pooled sets of 18 movements were analyzed per subject per target. If the intrinsic pattern of finger trajectories did not change across vision and speed conditions, the residual distance between any finger trajectory and the consensus would be the same in both individual and pooled analyses. Alternatively, finger trajectories with differing intrinsic patterns across experimental conditions would present larger residuals in the pooled than in the individual analyses. For each subject and target, six one-tailed paired *t*-test were used to compare the residuals of the same 18 movements calculated following individual and pooled GPA. One-tailed tests were used because residuals from pooled analyses were expected to be larger. A Bonferroni adjustment was applied to correct the family-wise error rate due to a given condition being involved in three comparisons. The same methods were repeated using joint trajectory data.

INTRINSIC VERSUS EXTERNAL FRAME OF REFERENCE FOR MOVEMENT PLANNING. This analysis was to determine whether movements are more simply characterized in an intrinsic or extrinsic reference frame. We expected minor differences between the two frames for movements to T2, which involved only slight trunk rotation, but substantial differences for T1 and T3, which involved large rotations of the torso. The maximal deviations of finger trajectories plotted in trunk-based coordinates were compared with those of trajectories plotted in external coordinates. The influence of the frame of reference on the maximal deviation was analyzed with univariate ANOVAs for repeated measures performed separately for each target. The velocity of reaching movements to the targets for fast and slow reaches was also plotted as a function of elapsed time. This allowed us to determine whether the velocity patterns would be most simply characterized, e.g., bell-shaped, in an intrinsic or external reference frame.

RESULTS

Patterns of reaching movements: illustrative data showing trajectories before and after GPA

Figure 1 shows the finger and joint trajectories of the nine reaching movements made by a typical subject to T1 in the DF condition. These movements required both arm projection and large trunk rotations. Figure 1 shows the trajectories in external space (*left, A*) and joint space (*C*) and shows the same data following GPA (*right*). To identify the consensus configuration during GPA, each finger or joint trajectory was translated and rotated by a different amount. Consequently, no single point in Fig. 1*B* corresponds, for example, to the location of the start position of the finger or to the position of the target (Fig. 1*A*, ■). The transformed trajectories are conventionally shown relative to the principal axes of the consensus configuration. To facilitate the interpretation of the three-dimensional joint trajectory data, two plane projections are shown in both the joint angle and principal axes coordinate systems.

Figure 1 illustrates several of the main findings concerning finger and joint trajectories obtained in the context of GPA. In external space (Fig. 1*A*), the finger did not reproduce the same trajectory on all nine reaches to a target in a given experimental condition. The trajectories varied in location and orientation, although the finger always began its motion from the same start position (the microswitch). The finger trajectories also varied in shape. Following GPA (Fig. 1*B*), the discrepancies between the trajectories were considerably reduced, indicating that much of the between-trial variability was extrinsic (i.e., in location and orientation) rather than intrinsic (i.e., in shape). In joint space (Fig. 1*C*), the trajectories did not originate from a single point because small inter-trial differences in initial body posture altered the elbow, shoulder, and trunk angles. Except for small joint reversals near the end of the movements, joint angle changes were generally monotonic during the reaches to T1, with leftward trunk rotation, shoulder flexion, and elbow extension occurring simultaneously. For T2, joint trajectories were mostly contained within the shoulder/elbow angle plane due to minimal trunk rotation involvement, while trajectories to T3 often exhibited reversals in the shoulder angle toward the end of the reaching movement (not shown). The differences between the trajectories in joint space were also substantially lessened by GPA and the transformed trajectories were largely contained in the plane defined by the first two principal axes of the consensus configuration (e.g., notice straight-line projections below and to the side of the trajectories to T1 in Fig. 1*D*).

To investigate compensation for interaction torques, we examined the effects of the speed and vision conditions on the intrinsic patterns of the finger and joint trajectories—i.e., on their entire shape irrespective of location and orientation variability in the external and joint workspaces. Figure 2 shows the finger (*top*) and joint (*bottom*) trajectories of nine reaching movements to T1 performed at two different speeds by another subject. The trajectories of individual movements made in the DS (*left*) and DF (*middle*) conditions are shown as well as the consensus configurations (*right*). For this subject, joint trajectories of DF movements were more curved and involved larger arm joint excursions than those of DS movements (compare the

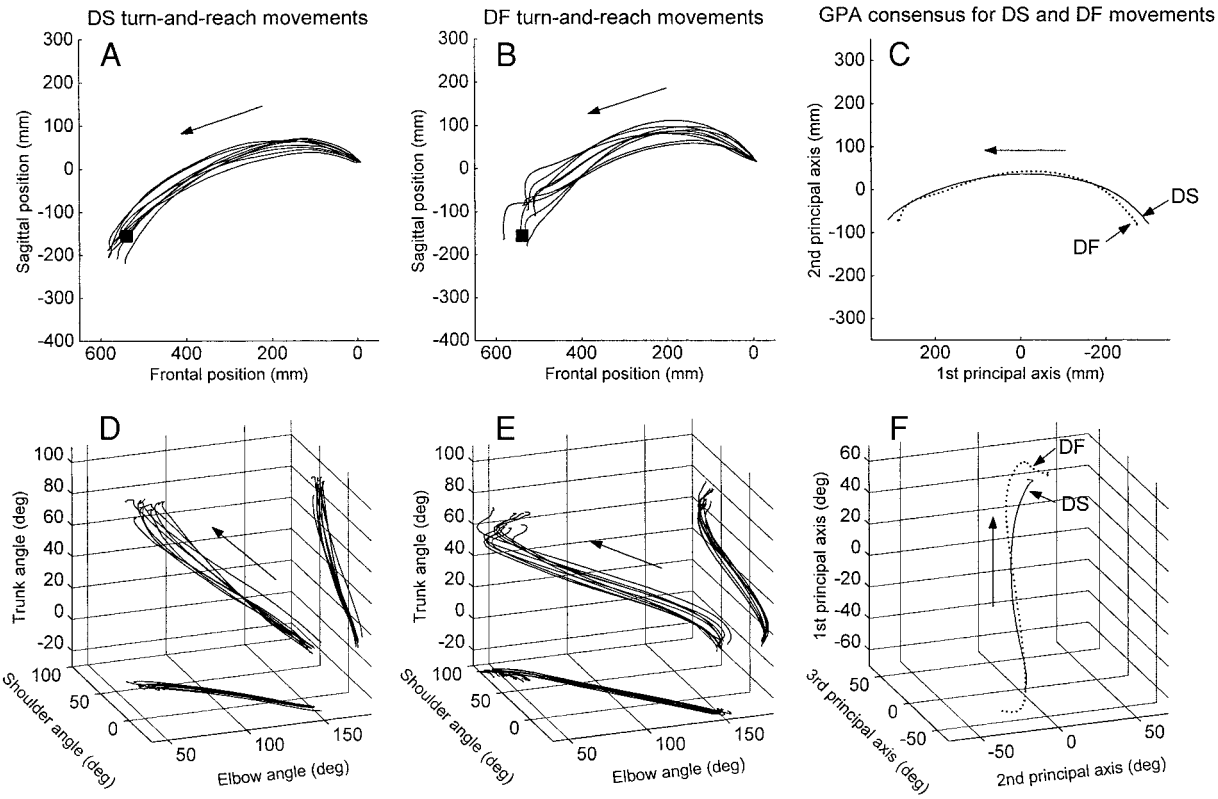

FIG. 2. Finger (*top*) and joint (*bottom*) trajectories of reaching movements to T1 performed by *subject S3*. *Left* and *middle*: the original trajectories performed in the dark-slow (DS) and DF conditions respectively. *Right*: the consensus configurations of the same movements for each condition (DS: —; DF: · ··). For clarity, 2 plane projections are shown for the original joint trajectories (*bottom left* and *middle*).

projections to the side and below the trajectories in Fig. 2, *D* and *E*). The consensus configuration obtained from joint data were thus considerably different for the two movement velocities (Fig. 2*F*). By contrast, the consensus configuration was rather similar for the two sets of finger trajectories (Fig. 2*C*).

Curvature of the consensus configuration: trajectories in external space are less affected than trajectories in joint space by changes in speed conditions

We initially analyzed the effects of speed and vision conditions on the intrinsic patterns of the trajectories using the curvature of the consensus configuration. Repeated-measures two-way ANOVAs were performed separately for each subject and target to identify potentially opposite effects in different subjects that would otherwise go undetected if group curvatures were analyzed. Figure 3 shows the effect of the change from the slow to fast speed condition (*left*) and from the light to dark vision condition (*right*) on the consensus configuration curvature of finger (*top*) and joint trajectories (*bottom*) for each target. In these figures, gray triangles indicate the magnitude, directionality, and generality of the significant effects of the factors. The base of each triangle corresponds to the mean curvature of movements performed in the slow or light condition, using values obtained from subjects exhibiting a significant speed or vision effect, respectively. Accordingly, the apex of each triangle is equal to the mean curvature of movements performed in the fast or dark condition in the same subjects. The width of the base of each triangle is scaled to the number of subjects (indicated in parentheses) exhibiting a significant effect of speed or vision where each tick mark represents one subject. Each triangle represents a different subset of the original seven subjects.

Significant effects of speed and vision conditions were found in both workspaces and for all targets. However, in our group of subjects, the most reliable effect observed was an increase in the curvature of joint trajectories following an increase in movement speed for the targets requiring substantial trunk rotation (T1,T3). ANOVAs performed on joint space data

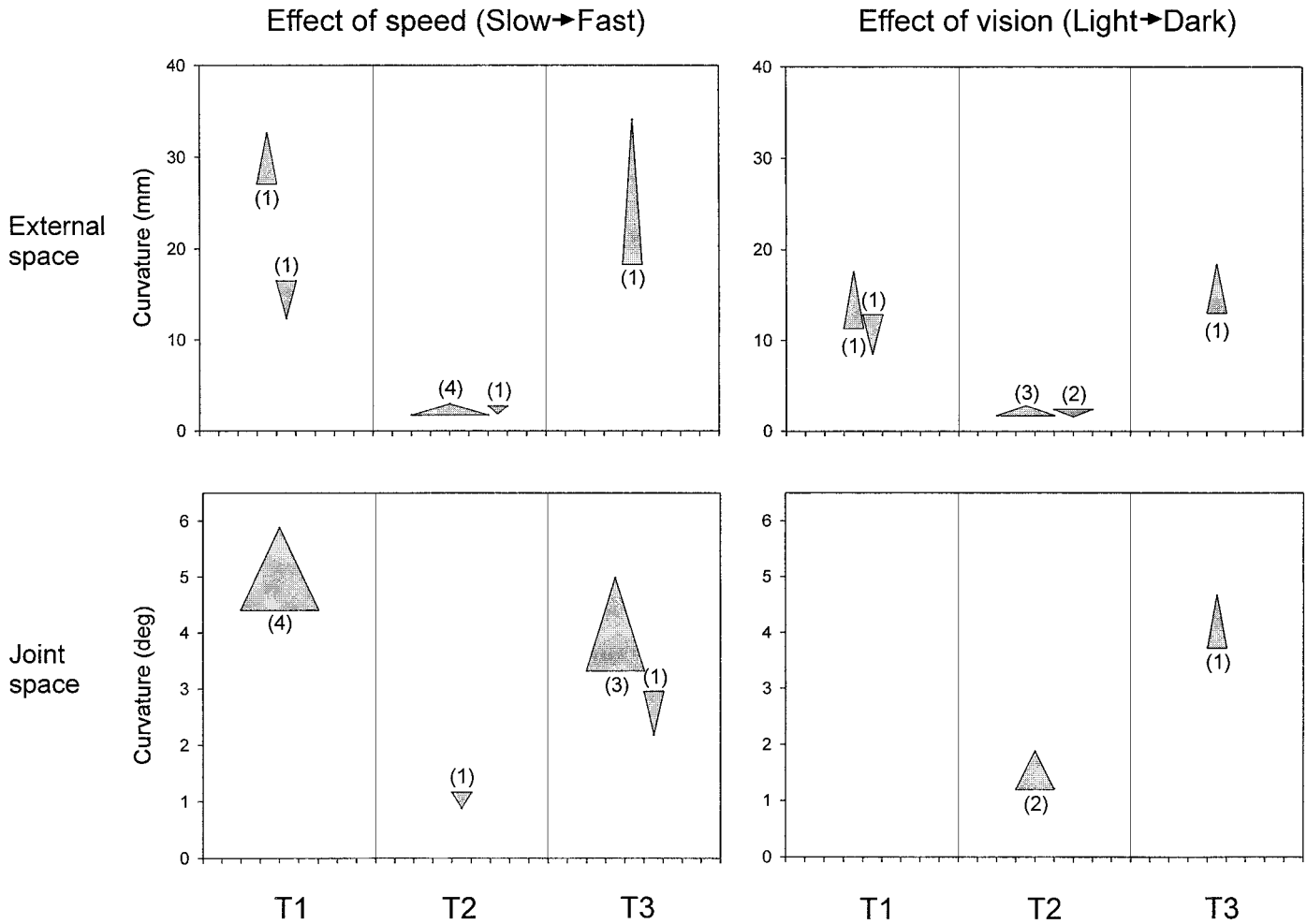

FIG. 3. Effect of the change from the slow to fast speed condition (*left*) and from the light to dark vision condition (*right*) on the consensus configuration curvature of external space (*top*) and joint space (*bottom*) trajectories. The base of each triangle corresponds to the mean curvature of movements performed in the slow (*left*) or light (*right*) conditions and the apex to the mean curvature of movements performed in the fast or dark conditions, using values obtained from subjects exhibiting a significant speed or vision effect. The number of such subjects (indicated in parentheses) is used to scale the base of each triangle where each tick mark represents 1 subject. For each target in each panel, a single triangle indicates that all significant changes in curvature were in the same direction, 2 triangles indicate that both significant increases and decreases in curvature were observed, and no triangle indicates that there were no significant effects.

revealed that the change from slow to fast reaching movements increased the consensus configuration curvature in four subjects for T1 [$F(1,240) > 6.1$, $P < 0.02$] and three subjects for T3 [$F(1,148) > 5.5$, $P < 0.02$], while it decreased the curvature in one subject for both T2 [$F(1,124) = 4.3$, $P < 0.04$] and T3 [$F(1,148) = 9.5$, $P < 0.01$; Fig. 3, *bottom left*]. In external space, the finger trajectories to T1 and T3 were less systematically affected by the change from slow to fast movements, with one subject showing an increase for both T1 [$F(1,240) = 5.4$, $P < 0.03$] and T3 [$F(1,148) = 39.4$, $P < 0.01$] and one subject a decrease for T1 [$F(1,240) = 10.4$, $P < 0.01$] in consensus configuration curvature. For T2, the (relatively straight) finger trajectories were more curved in fast than in slow movements in four subjects [$F(1,124) > 8.2$, $P < 0.01$] and less so for one subject [$F(1,124) = 9.5$, $P < 0.01$; Fig. 3, *top left*]. In joint space, the removal of visual feedback increased the consensus configuration curvature in two subjects for T2 [$F(1,124) > 13.6$, $P < 0.01$] and one subject for T3 [$F(1,148) = 6.2$, $P < 0.02$; Fig. 3, *bottom right*]. In external space, the effect of removing visual feedback on the finger trajectories to T1 and T3 was variable, with one subject showing an increase for both T1 [$F(1,240) = 23.4$, $P < 0.01$] and T3 [$F(1,148) = 10.3$, $P < 0.01$] and one subject a decrease for T1 [$F(1,240) = 14.9$, $P < 0.01$] in consensus configuration curvature. For T2, the finger trajectories were more curved in the dark than light vision condition in three subjects [$F(1,124) > 5.8$, $P < 0.02$] and less so in two subjects [$F(1,124) > 6.0$, $P < 0.02$; Fig. 3, *top right*].

RMS residual distances to the consensus configuration show smaller increases in external space than joint space coordinates following pooling across speed conditions

Two configurations with similar curvature values may actually have different shapes (Haggard and Richardson 1996). Therefore in a second analysis, we examined the shapes of finger and joint trajectories across speed and vision conditions using the residual rms distances between the transformed trajectories and the consensus configuration. For each target, residuals were calculated after GPA was applied both individually to sets of nine movements performed in two different experimental conditions, and following the pooling of the same 18 movements. A significant increase in the residuals subsequent to pooling would indicate that significantly different intrinsic patterns (i.e., shapes) of trajectories were associated with the two conditions. For each subject, the *t* values of the six tests performed on the residuals obtained from external and joint space data to T1 (the target requiring both arm projection and substantial trunk rotation) are reported in Table 1, with values larger than the critical $t(17)$ value of 2.338 shown in bold type. External and joint space residuals data for all three targets are shown in Fig. 4 using a format similar to that used for Fig. 3. In this case, gray triangles indicate the magnitude and generality of the significant increases in residuals due to pooling across experimental conditions. The base of each triangle corresponds to the mean external (*top*) or joint space residuals (*bottom*) prior to pooling across speed (*left*), vision (*middle*), or both conditions (*right*), whereas the apex of each triangle is equal to the mean residuals after pooling. The mean values were calculated using data from only those subjects whose residuals significantly increased following pooling. Because each type of pooling involved two separate *t*-test per subject (e.g., testing the effect of speed involved *t*-test comparing the residuals of LS/LF and DS/DF trials before and after pooling), a total of 14 significant comparisons were possible per target (7 subjects each contributing ≤2 significant *t*-tests). The base of each triangle was scaled to reflect the number of significant comparisons (of a maximum of 14) per type of pooling. Note that each tick mark now represents two significant comparisons, which may or may not have been contributed by the same subject. For example, the two significant increases in external space residuals to T2 observed when pooling across speed (Fig. 4, *top left*) were contributed by two different subjects, both for the LS/LF comparison. The two numbers under each triangle respectively indicate the total number of significant comparisons for that target and type of pooling and the total number of subjects that contributed at least one significant comparison. Because we were most interested in the intrinsic patterns of finger and joint trajectories of movements involving both arm extension and substantial trunk rotation, we will focus our discussion on the analysis of residuals obtained in reaches to T1 (Table 1 and Fig. 4).

TABLE 1. *Values of t(17) for comparing rms residuals of each finger or joint trajectory from the consensus configuration of its own condition with the rms residuals from the consensus configuration when analyzed jointly with a second condition*

	External Space (First Condition)				Joint Space (Second Condition)			
	LS	LF	DS	DF	LS	LF	DS	DF
S1								
LS	—				—			
LF	0.82	—			**3.49**	—		
DS	**2.71**	1.94	—		1.19	**3.54**	—	
DF	**3.90**	2.14	0.83	—	**3.29**	1.18	**3.14**	—
S2								
LS	—				—			
LF	1.47	—			**3.35**	—		
DS	−0.01	2.32	—		**3.20**	**3.85**	—	
DF	2.09	1.48	0.82	—	1.72	1.67	**3.74**	—
S3								
LS	—				—			
LF	2.12	—			**5.99**	—		
DS	1.34	1.65	—		1.32	**13.52**	—	
DF	1.66	1.82	**3.01**	—	**5.81**	1.71	**12.54**	
S4								
LS	—				—			
LF	1.62	—			**3.96**	—		
DS	1.35	1.46	—		**4.42**	0.78	—	
DF	**2.49**	2.26	1.42	—	**4.69**	1.55	1.80	—
S5								
LS	—				—			
LF	1.72	—			2.06	—		
DS	1.30	**3.24**	—		**4.27**	**2.92**	—	
DF	0.87	**2.67**	0.94	—	**3.00**	2.16	2.26	—
S6								
LS	—				—			
LF	1.43	—			**4.63**	—		
DS	**3.26**	1.46	—		1.61	**6.51**	—	
DF	**3.01**	0.77	1.49	—	**2.38**	2.04	**3.25**	—
S7								
LS	—				—			
LF	1.76	—			**4.85**	—		
DS	0.68	1.07	—		**2.82**	**3.07**	—	
DF	1.90	1.56	1.68	—	2.30	1.51	1.21	—

Values in bold type are above the critical 2.338 value and are significant at the 0.05 level after Bonferroni adjustment. L, light; D, dark; S, slow; F, fast; *S1, subject 1;* rms, root mean square.

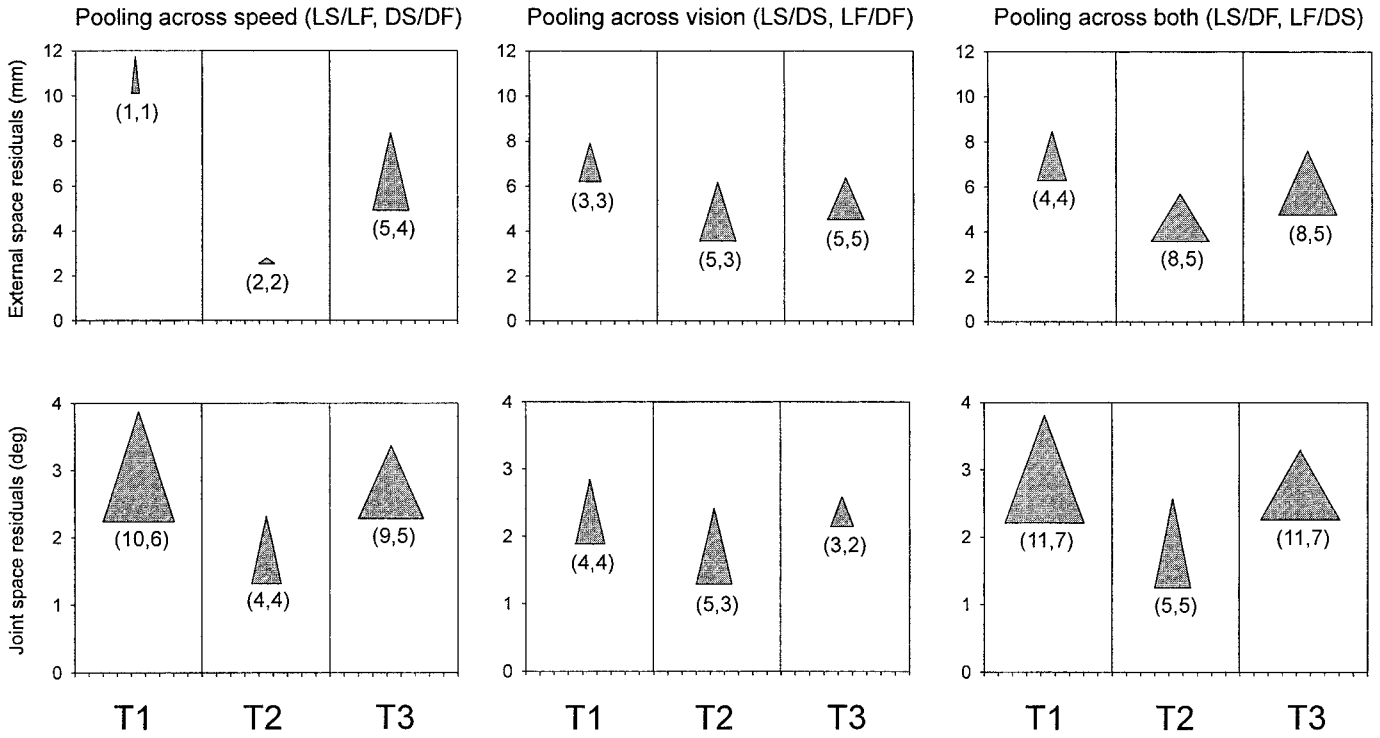

FIG. 4. Effect of pooling the external space (*top*) and joint space (*bottom*) trajectories across speed (*left*), vision (*middle*), or both conditions (*right*) on the residual distances to the consensus configuration following GPA The base and apex of each triangle correspond to the mean root-mean-square (rms) residuals prior to and after pooling for those subjects exhibiting a significant effect of pooling. The total number of significant comparisons and total number of subjects that contributed ≥1 significant comparison are indicated under each triangle, with the former number used to scale the triangle base. Each tick mark indicates 2 significant comparisons which may or may not have been contributed by the same subject.

When joint trajectories to T1 were pooled together across differing speed conditions (*right side* of Table 1, LS/LF and DS/DF *t*-test), the residual distances to the consensus configuration increased significantly in 10 of 14 comparisons (contributed by 6 different subjects) in which the mean residual increased 72% from 2.24 to 3.86° (Fig. 4, leftmost triangle in *bottom left*). The same pooling for finger trajectories to T1 (*left side* of Table 1) gave rise to only one significant comparison in which the mean residual increased just 16% (from 10.13 to 11.71 mm; Fig. 4, leftmost triangle in *top left*). This means that most subjects used a different pattern of interjoint coordination in slow and fast movements but did not substantially change the shape of their finger trajectory, a finding consistent with the fact that, in several subjects, the consensus configuration curvature of reaching movements to T1 was sensitive to speed in joint space but not external space (Fig. 3).[1] Vision conditions affected the intrinsic patterns of finger and joint trajectories to T1 to a similar but modest degree, with respectively three and four significant comparisons for external and joint space data (Table 1, LS/DS and LF/DF *t*-test). In those comparisons, pooling across vision conditions increased the mean amplitude of external space residuals from 6.22 to 7.91 mm and of joint space residuals from 1.89 to 2.84° (Fig. 4, left-most triangles in *top middle* and *bottom middle*). Finally, when the speed and vision conditions of the two sets of movements to T1 were both different (*right side* of Table 1, LS/DF and LF/DS *t*-test), the joint space residuals of pooled analyses were significantly greater than those of individual analyses in 11 of 14 comparisons (contributed by all 7 subjects), in which the mean residual increased 72% from 2.21 to 3.80° (Fig. 4, leftmost triangle in *bottom right*). Conversely, the external space residuals were greater in the pooled analyses only in four comparisons, in which mean residual increased 34% from 6.30 to 8.44 mm (Fig. 4, leftmost triangle in *top right*). The analysis of trajectories pooled across both speed and vision conditions strengthens the results of the single-factor poolings by suggesting a cumulative effect of the two factors. Indeed, with joint and finger trajectories similarly sensitive to the vision factor, the larger number of significant comparisons in joint space emphasizes that speed had a larger impact on the interjoint coordination than on the finger trajectory.

The analysis of finger and joint trajectories to T2 and T3 (Fig. 4, middle and right-most triangles in all panels) revealed generally similar results, with pooling across speed being more frequently associated to significant increases in residuals in joint than external space, and pooling across vision having comparable effects in both coordinate spaces. Pooling across both conditions showed a more generalized impact in joint than external space for reaches to T3 but not to T2.

[1] Our study cannot address the impact of speed upon final *postures* following turn-and-reach movements because our subjects could vary their initial posture between speed conditions. Recent studies of reaching movements in three-dimensional space have described final arm postures as dependent on initial arm postures (Soechting et al. 1995) but not movement speed (Nishikawa et al. 1999) and hypothesized that the minimization of kinetic energy determines final arm postures. Modeling studies of sagittal reaching movements involving the hip, shoulder, and elbow joints have suggested that when the target is within the work space, movement speed may influence individual joint contributions, with that of the large trunk segment being proportionally smaller at high than low speed (Rosenbaum et al. 1993).

Joint peak velocities and accelerations were unaffected by trunk movement speed

To determine whether the larger Coriolis, centripetal, and inertial torques induced by rapid trunk rotation might interfere with arm joint rotations, we examined the joint velocity and acceleration profiles of slow and fast turn-and-reach movements. The mean kinematic data of nine reaching movements to T1 performed by one subject were used to calculate the joint velocity and acceleration profiles of trunk rotation, shoulder flexion and elbow extension in the LS and LF conditions. These profiles are presented in Fig. 5. Although all three joint angles reached higher peak velocities in the fast condition, the increase was proportionally greater for the arm joints than for the trunk (compare *A* and *B*). For the subjects as a group, the ratio of peak shoulder to peak trunk angular velocities was 1.74 for slow and 2.76 for fast movements to T1, whereas that of peak elbow to peak trunk angular velocities was 1.52 and 2.30, respectively. Similar ratios using acceleration data revealed that, in fast movements to T1, the arm joint rotations had peak acceleration values that were nearly four times those of trunk rotation. Both the shoulder/trunk and elbow/trunk peak acceleration ratios increased significantly between the slow and fast conditions [$F(1,6) > 6.62$, $P < 0.05$; Fig. 5, *C* and *D*]. The shoulder joint accelerated for a proportionally longer time in the fast movement conditions, reaching its peak acceleration at 92% of the time to peak trunk acceleration versus 74% in slow movements [$F(1,6) = 8.05$, $P < 0.03$]. Similarly, the shoulder velocity reached its peak at 77 and 71% of the time to peak trunk velocity in fast and slow movements, respectively [$F(1,6) = 7.45$, $P < 0.04$]. The peak elbow acceleration and velocity were similarly timed across speed conditions. Taken together, these results indicate that larger trunk rotation induced torques at higher movement speeds did not impede the arm joint rotations.

Internal versus external frames of reference for movement planning: present evidence favors external frame

The second goal of these experiments was to identify the frame of reference in which turn-and-reach movements could be most simply described. Typical finger trajectories and velocity profiles of one subject's slow and fast reaching movements performed with visual feedback to the three targets are shown in Fig. 6 in external (*left*) and internal or trunk-based coordinates (*right*). In Fig. 7, the finger trajectories of all reaching movements performed by the same subject (*S5*) in all experimental conditions are plotted relative to a trunk-based frame of reference.

From the viewpoint of the rotating trunk, the finger trajectory to T1 was bow-shaped, with the finger moving away and to the left before curving back toward the body midline as the trunk continued to rotate leftwards (Figs. 6, *right*, and 7). Because little trunk rotation was used to reach T2, the finger trajectory to this target remained relatively similar across the two reference frames, although the characteristic leftward curvature was also observed in trunk-based coordinates. Finger trajectories to T1 and T2 observed in trunk-based coordinates

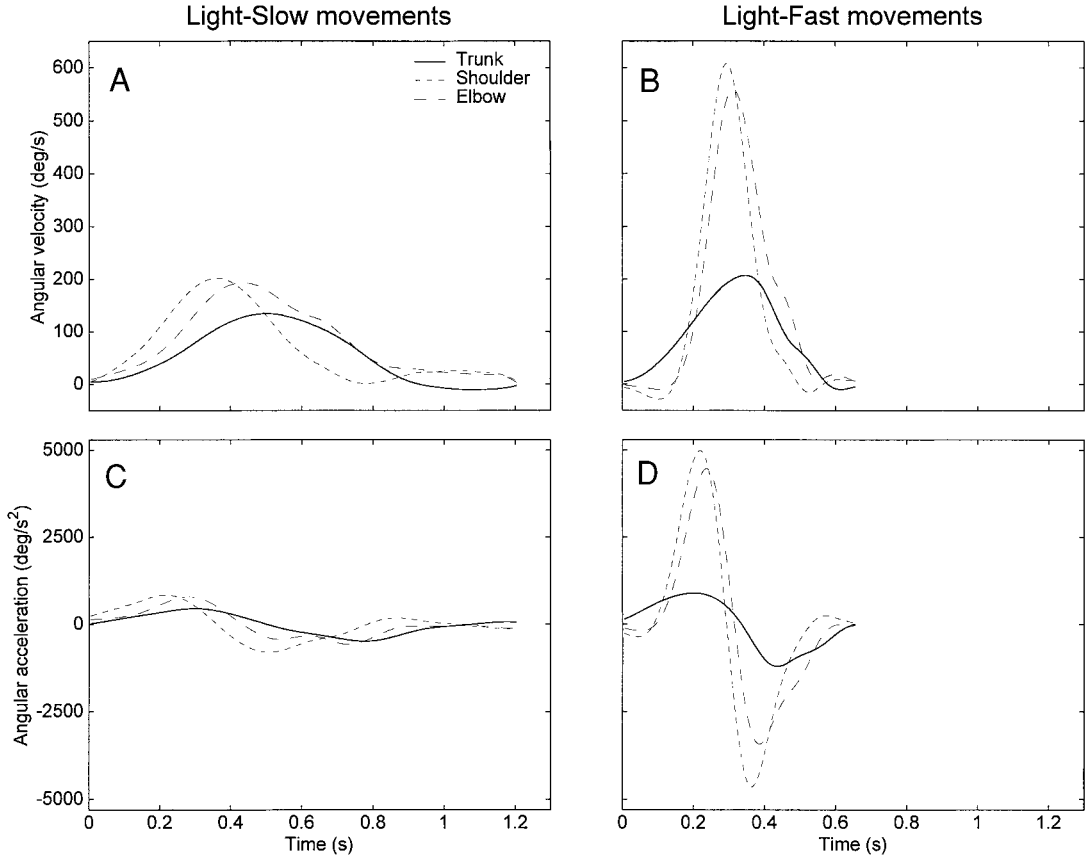

FIG. 5. Trunk, shoulder, and elbow angular velocity (*top*) and acceleration (*bottom*) profiles of averaged reaching movements to T1 performed by *subject S7* in the light-slow (LS; *left*) and light-fast (LF; *right*) conditions.

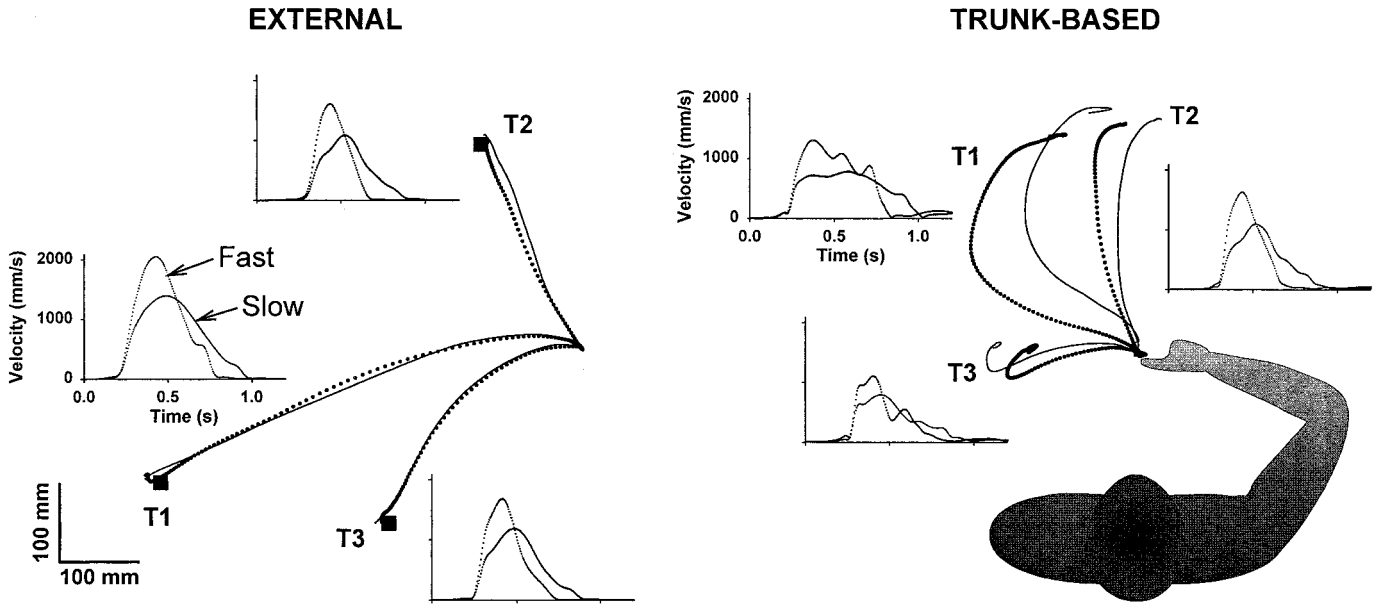

FIG. 6. Typical finger trajectories and velocity profiles of *subject S5* performing slow (—) and fast (· · ·) reaching movements with visual feedback to the 3 targets in an external (*left*) and trunk-based reference frame (*right*). ■, the target locations in external coordinates. In trunk-based coordinates, the target locations draw nearer to the body as the trunk rotates and are thus not shown. Rather, the symbols identify each pair of finger trajectories associated with each target of the reaching movements.

generally ended near each other (Figs. 6, *right*, and 7), indicating that the final arm configuration relative to the trunk was similar for both targets as had been intended when selecting their positions. For movements to T3, the finger trajectory in trunk-based coordinates was mostly leftward, with a small reversal in direction visible for most subjects near the end.

For T1 and T2, the maximal trajectory deviation, across subjects, was greater using trunk-based coordinates [$F(1,6) > 12.8$, $P < 0.02$; mean of −105 and −39 mm, respectively], and in this reference frame, the deviations were to the left of the line joining the endpoints of the finger trajectory and generally occurred near the time of peak trunk angular velocity (Fig. 7, ●). For T3, maximal trajectory deviations in trunk-based coordinates could occur on either side of this line, but were of

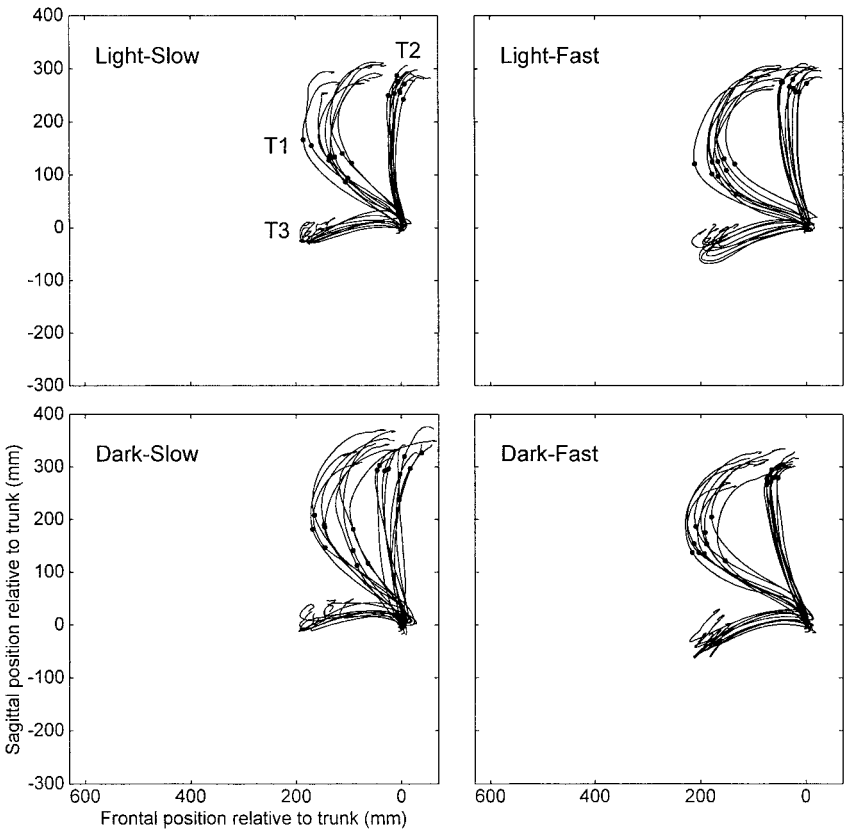

FIG. 7. Finger trajectories of the movements performed by *subject S5* in each experimental condition seen from a trunk-based frame of reference. ● [on the trajectories of movements involving significant finger displacement away from the trunk (T1 and T2)], the finger location at the time of peak trunk angular velocity. For clarity, the initial position of the finger in the trunk-based reference frame (~200 mm in the sagittal plane, ~0 mm in the frontal plane) has been subtracted from the finger position data such that all trajectories begin near (0,0).

smaller magnitude than in external coordinates [$F(1,6) = 25.5$, $P < 0.01$, unsigned mean of 33 mm]. The magnitude of the deviations in trunk-based coordinates did not vary significantly across vision or speed conditions for any of the targets ($P > 0.05$), although for T1, deviations were 33% larger in fast than in slow movements (−120.1 and −90.53 mm, respectively; compare the trajectories to T1 in Fig. 7, *left* and *right*). Larger leftward deviations of the finger from the body midline were consistent with subjects generating greater arm extensions and using a larger portion of the joint workspace in fast than slow reaches to T1 (e.g., Fig. 2, *D* and *E*), as were the increased consensus configuration curvatures of joint trajectories in several subjects (Fig. 3, *bottom left*). However, because not all subjects exhibited a sensitivity to speed in their joint trajectories to T1, we tested the effect of movement speed on maximal trajectory deviations to this target on an individual basis. In trunk-based coordinates, four subjects had significantly larger maximal trajectory deviations in fast than in slow movements [means for these subjects: −133.72 and −81.91 mm, respectively; $F(1,8) > 12.59$, $P < 0.01$]; these were the same subjects that displayed larger consensus configuration curvatures in fast movements to T1. In external coordinates, one subject exhibited significantly smaller maximal trajectory deviations in fast than in slow movements to T1 [51.13 and 65.97 mm, respectively; $F(1,8) = 21.64$, $P < 0.01$].

For all three targets and both movement speeds, finger velocity profiles in external coordinates were basically bell-shaped with occasionally a slightly prolonged deceleration phase (Fig. 6, *left*). In contrast, finger velocity profiles for movements to T1 and T3 based on trunk-based coordinates often had multiple peaks or a flattened appearance (Fig. 6, *right*). Because the trunk moved only slightly when subjects reached to T2, the finger velocity profile was nearly the same in external and trunk-based finger coordinates.

To assess the differences in the velocity profiles between the two reference frames, each set of nine velocity profiles produced by the same subject in the same experimental condition was scaled in duration and amplitude to its mean values and averaged. The resulting mean velocity profiles (± SD) of movements performed by *S2* with visual feedback to the three targets are shown in Fig. 8 both in external (*top*) and trunk-based coordinates (*bottom*). In all subjects and for both movement speeds, the profiles for T1 and T3 were less smooth in trunk-based than in external coordinates, while those to T2 appeared similar across both frames of reference. Repeated-measures ANOVAs revealed that the peak SD of each profile (normalized to the peak velocity) was significantly larger in trunk-based than in external coordinates for movements to T1 and T3 [$F(1,6) > 22.01$, $P < 0.01$; compare the width of the dashed lines for T1 and T3 in Fig. 8, *top* and *bottom*] but not T2 ($P > 0.08$). Thus when reaching movements involved significant trunk rotation, their finger velocity profiles were more stereotypical when calculated in an external frame of reference.

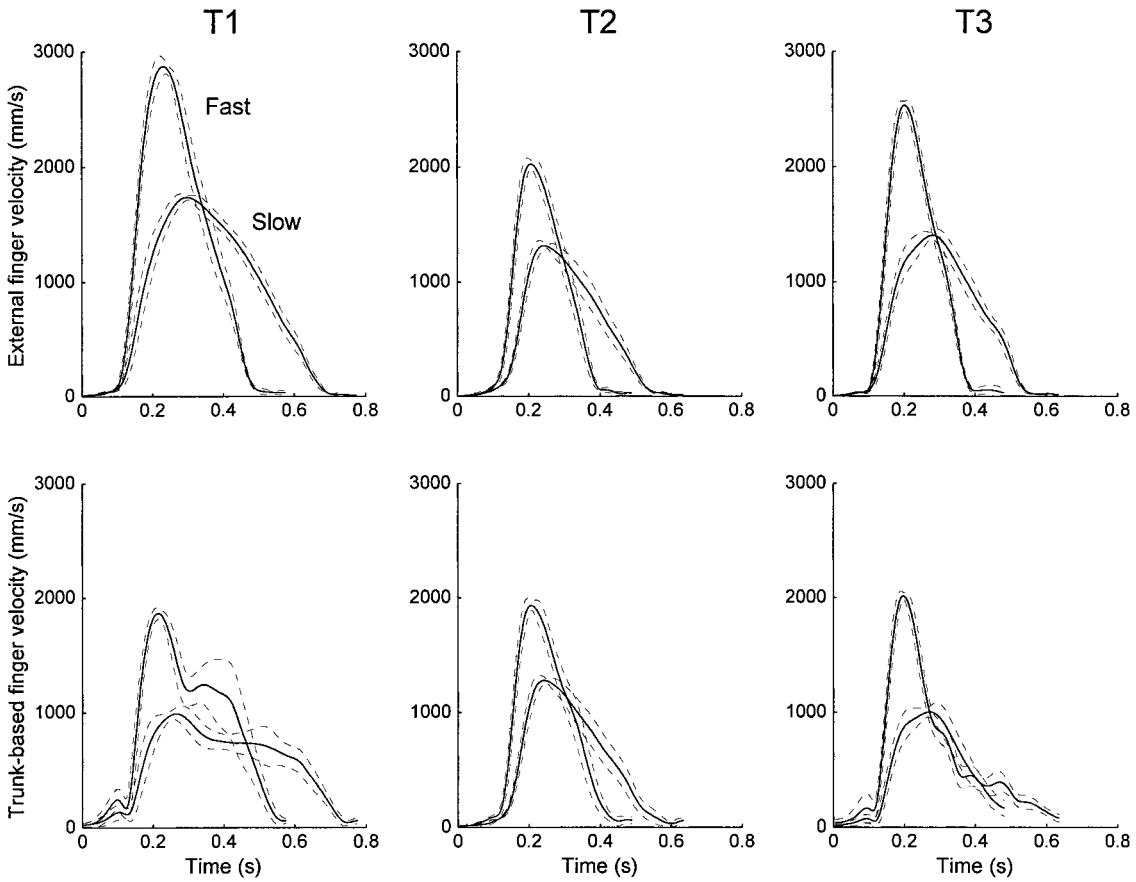

FIG. 8. Mean velocity profiles (±SD) of movements performed by *S2* with visual feedback to the 3 targets in external (*top*) and trunk-based coordinates (*bottom*).

DISCUSSION

We had two basic goals: to determine the influence of interaction torque magnitude and of visual feedback on the trajectories of reaching movements made during simultaneous trunk rotation and to identify the reference frame in which turn-and-reach movements could most parsimoniously be described. We analyze below our findings that lead us to conclude, first, that the CNS anticipates and compensates precisely for self-generated interaction torques and, second, that the central representation of movement parameters must include specifications in relation to an extrinsic reference frame.

To achieve the first goal we made use of GPA (cf. Haggard and Richardson 1996; Haggard et al. 1995). The discrepancies between trajectories of repeated movements to each target represented in both external and joint space were greatly reduced following GPA, indicating that much of the trajectory variation in external space was due to the finger landing in different places and that much of the variation in joint space resulted from slightly different start configurations and different final configurations. GPA effectively identifies and eliminates this extrinsic variability.

We initially considered the curvature of the consensus configuration of trajectories of reaching movements to the three targets and how it was affected by speed and visual feedback in individual subjects. For movements to T1, we found that joint trajectories were more curved in fast than slow movements for most subjects, whereas the effect of speed on finger trajectories was variable and limited to a few subjects. In either workspace, the effect of removing visual feedback on the trajectories to T1 was also variable and limited to a few subjects. The effects of speed and vision conditions on joint and finger trajectories to T2 and T3 were generally similar to those for T1 except that joint trajectories to T2 exhibited little effect of speed on their curvature. We then calculated for individual subjects the rms residuals following GPA for sets of nine movements for given conditions and for sets of 18 movements across two conditions. The comparisons between the residuals from individual and pooled analyses of movements to T1 indicated once more that movement speed had a large effect on the shape of joint trajectories but very little effect on that of finger trajectories. Visual feedback had a similar modest influence on finger and joint trajectories to T1 as well as on those to the other targets. For T2 and T3, movement speed again showed a larger effect on joint than finger trajectories, although not as sharply pronounced as that observed for T1. Finally, by calculating the ratios of shoulder to trunk and elbow to trunk peak angular velocities for slow and fast turn-and-reach movements, we established that the greater interaction torques associated with faster trunk rotations did not lead to impeded or retarded arm joint rotations.

Effect of movement speed on external and joint space trajectories

Previous investigations of reaching in the sagittal plane and in three-dimensional space (Atkeson and Hollerbach 1985; Hong et al. 1994; Lacquaniti et al. 1986; Nishikawa et al. 1999; Soechting and Lacquaniti 1981) and of whole-body reaching combining an arm movement with a forward step (Flanders et al. 1999) demonstrated that hand or wrist paths are generally independent of the speed at which they are performed (although see Pozzo et al. 1998, 2002). Similarly, horizontal projections of finger trajectories in most of our subjects were of comparable curvature and overall shape across speed conditions, even as trunk rotation contributed substantially to the finger displacement.

Our results conflict with the hypothesis that the CNS keeps arm trajectory kinematics independent of speed by using a scaling strategy in which the rate-dependent and gravity components of torque profiles are generated by two separate force drives that can be separately scaled (Hollerbach and Flash 1982). Indeed, according to this hypothesis, a movement is produced r times faster by simply scaling the rate-dependent components of the torque profiles by r^2, an operation that should not affect the interjoint coordination. In contrast, our analysis of turn-and-reach movements revealed a differential effect of speed on joint coordination in several subjects wherein the trunk, shoulder, and elbow joint rotations of fast movements generally occupied a larger portion of the joint workspace than those of slow movements. Similarly, a recent study examining the effect of movement speed on the joint angle profiles of seated subjects performing reaching movements concluded that the scaling effect of movement time or average speed, in a strict sense, was not present in the joint kinematics (Zhang and Chaffin 1999). Therefore according to these and our own findings, a fast movement may not strictly consist of a sped up version of the same movement performed at slow speed, at least in terms of its joint coordination.

Kinematic redundancy

Kinematic redundancy was present during our turn-and-reach movements: 3 df (trunk rotation, shoulder flexion, and elbow extension) jointly contributed to the location of the finger at each point along its trajectory between the start and end positions on the table. Theoretically, the kinematic redundancy of the human upper limb allows different interjoint coordinations and different endpoint trajectories to move the hand between two locations in space, an ability termed "motor equivalence" (Bernstein 1967; Lashley 1930). Situations in which joint redundancy of the upper limb is commonly exploited include postural pointing tasks (Morrison and Newell 1996), double-step paradigms (Robertson and Miall 1997), and obstacle avoidance tasks (Dean and Brüwer 1994). Our finding that several subjects used different interjoint coordination patterns at different reaching speeds to produce the same finger trajectory indicates that joint redundancy may also be exploited in the context of turn-and-reach movements.

Motor equivalence does not rule out stereotyped patterns in external or joint space kinematics when a movement is performed in a reproducible context. However, the fact that, in several subjects, an increase in movement speed had an impact on the interjoint coordination but not the finger trajectory indicates a precedence in preserving the latter over the former. Similarly, other studies have reported that several features of the hand path and of grasp are preserved at the behavioral level when an arm reaching movement is combined with trunk flexion (Ma and Feldman 1995; Pigeon et al. 2000; Wang and Stelmach 1998) or locomotion (Cockell et al. 1995; Marteniuk et al. 2000) despite changes in the intrinsic coordinates. Thus joint redundancy may not only contribute to the successful performance of a task, but may also be used to preserve the

extrinsic—rather than intrinsic—features of a reaching movement when, for instance, the recruitment of additional degrees of freedom compels the arm to move relative to a nonstationary base of support.

Our analysis of joint kinematics during turn-and-reach movements also indicates that when the dynamical demands of a task exceed the physiological capabilities required to maintain a given motor coordination, a more extensive use is made of the arm/trunk joint workspace. For example, whereas elbow, shoulder, and trunk rotations generally varied monotonically in slow movements, several subjects exhibited joint reversals and momentary joint freezings in their fast turn-and-reach movements (e.g., compare the trunk/shoulder coordination in Fig. 2, *D* and *E*). This may explain the more curved joint consensus configurations of fast movements to T1 and the intrinsically different joint trajectory shapes associated with the different speed conditions observed in several subjects. Our analysis of peak joint velocity and acceleration ratios indicated that the overall change in joint coordination was due to arm segments moving proportionately faster relative to the trunk in fast than in slow turn-and-reach movements. The trunk's large inertia may prevent trunk rotation from keeping abreast of the arm joint acceleration profiles and cause the trunk motion to lag slightly behind that of the arm. Rather than slowing down the rotation speed of the shoulder and elbow joints to compensate for the trunk lag, subjects prevent an impact on the finger trajectory by modifying the angular excursions of the shoulder and elbow (compare Fig. 2, *D* and *E*).

Frames of reference for turn-and-reach movements

Well-known invariant features of natural reaching movements in hand space such as relatively straight paths and single-peaked bell-shaped velocity profiles suggest that movement planning occurs in an extrinsic frame of reference (Flash and Hogan 1985; Gordon et al. 1994; Morasso 1981). Kinematic and dynamic perturbation studies have provided additional support for this hypothesis by showing that movements tend to recover preperturbation kinematics such as straight-line hand paths following adaptation (Flanagan and Rao 1995; Lackner and Dizio 1994; Shadmehr and Mussa-Ivaldi 1994; Wolpert et al. 1995). In contrast, other findings such as the sizable curvature of hand paths in certain directions (Atkeson and Hollerbach 1985; Haggard and Richardson 1996) suggest that intrinsic or joint-based factors may also play a role in movement planning.

We examined the issue of planning in external versus internal (trunk-based) coordinates by looking at finger movement patterns and velocity profiles for the different target locations. In movements to T1 and T2, we found that finger trajectories had larger curvatures in trunk-based than external coordinates although not in movements to T3. In an external frame of reference, the deviations of trajectories to T1 were similar regardless of speed in all but one subject (whose deviations were actually smaller in the fast than slow movements), whereas from a trunk-based perspective, the deviations were larger in fast than in slow movements for four subjects. Although the final arm configuration relative to the trunk was similar for targets T1 and T2, the trajectory of the finger relative to the trunk varied depending on the contribution of trunk rotation to the movement. In the velocity domain, both slow and fast movements had basically bell-shaped velocity profiles in external space. By contrast, in trunk-based coordinates, velocity profiles of movements involving significant trunk rotation were multi-peaked or flattened in appearance, and exhibited greater variability. All but one[2] of these findings argue against trunk-based planning and implementation of turn-and-reach movements. Rather they suggest that the movement control respects an external frame of reference, where finger velocity profiles remain smooth and finger trajectory curvature is kept minimal (but not eliminated, particularly when trunk rotation contributes substantially to the movement) and insensitive to movement speed.

Cortical representation of reaching movements: extrinsic and intrinsic representations

The analysis of cell activity in the cerebral cortex of awake behaving monkeys has provided considerable insight regarding the frames of reference, parameter spaces, and coordinate transformations underlying reaching movements (for a review, see Kalaska et al. 1997). In particular, findings of a covariation of neural activity in primary motor cortex (M1) at the single-cell and population level with the direction and velocity of hand movement support the view that M1 generates a representation of movement in an extrinsic frame of reference centered on the hand (Georgopoulos et al. 1982, 1988; Schwartz 1992, 1993). Other studies have shown that the activity of individual neurons in M1 and dorsal premotor cortex during reaching movements is sensitive to intrinsic parameters such as arm orientation (Caminiti et al. 1990, 1991; Kakei et al. 1999; Scott and Kalaska 1997; Scott et al. 1997) and load conditions (Kalaska et al. 1989). The latter studies thus suggest that precentral cortical cells contribute to the control of reaching movements presumably after the extrinsic representation of the hand path or target location in space has been transformed into an intrinsic representation in terms of the mechanics of the arm.

A recent study of ventral premotor cortex shows directional tuning of cells to movements in an extrinsic frame of reference irrespective of forearm orientation (Kakei et al. 2001). Cells in M1 of the same animal by contrast showed modulations related to forearm orientations. These authors suggest that interactions between the ventral premotor area and M1 may be involved in generating the ". . .sensorimotor transformation between extrinsic and intrinsic coordinate frames." Our findings are consistent with this viewpoint and emphasize the need to take into account motion of the trunk in computing the intrinsic dynamic representation of the arm.

Our finding that turn-and-reach movements were most simply described in an external frame of reference does not imply that their control or representation at cortical levels occurs solely in extrinsic coordinates. It suggests, however, that the control of reaching movements involving trunk rotation prob-

[2] The one finding consistent with trunk-based planning is that of larger trajectory deviations in external than trunk-based coordinates in movements to T3. However, trunk-based deviations to T3 were variably distributed on either side of the line joining the ends of the trajectory, which itself appeared generally erratic (Fig. 7), exhibiting sharp turns and loops rather than a monotonic arc. Larger deviations in external space may partly result out of concern of the hand coming in too close proximity to the trunk. Taken together, these considerations suggest that the control of reaching movements to T3 may also occur in an external frame of reference.

ably occurs in coordinates other than or in addition to those of the trunk because body-relative trajectories to targets at similar body-relative final locations were sensitive to two intrinsic experimental factors (movement speed and the contribution of trunk rotation to the movement). Consistent with this perspective is the finding that in reaching experiments with monkeys, the neuronal activity in area 5 of posterior parietal cortex correlates poorly with target location expressed in body coordinates (Buneo et al. 2002). Moreover, in our experiments, the putative frame of reference attached to the body rotated as subjects recruited trunk rotation to reach the targets, thus generating additional interaction torques on the arm. Investigations of different patient populations have provided evidence that proprioception (Sainburg et al. 1995; Seidler et al. 2001), the cerebellum (Bastian et al. 1996, 2000; Topka et al. 1998), and the frontal cortex (Beer et al. 2000) play a role in the control of interaction torques. In addition, the planning of reaching movements must involve consideration of the external loads imposed by objects that are being controlled and the additional interaction torques associated with moving them.

In summary, our overall pattern of results indicates that the magnitude of self-generated interaction torques has virtually no influence on movement trajectories in external space either in terms of curvature or accuracy. The influence of speed on the variability of joint space trajectories is not due to larger interaction torques retarding arm joint rotations; in fact, these rotations are of higher velocity with higher trunk velocity. Instead, subjects utilize the "extra degrees of freedom" of the arm to achieve comparable external trajectories. This means that subjects, when making turn-and-reach movements, preplan appropriate compensatory joint torques to prevent the self-generated interaction torques from disturbing the path of the hand. It is clear the nervous system's task is simplified if the movements are controlled in relation to an external frame of reference. An upcoming paper (unpublished data) will provide a quantitative analysis and computation of the actual joint torques generated during turn-and-reach movements.

P. Pigeon was supported by a Postdoctoral Research Fellowship from the Natural Sciences and Engineering Research Council of Canada.

REFERENCES

Atkeson CG and Hollerbach JM. Kinematic features of unrestrained vertical arm movements. *J Neurosci* 5: 2318–2330, 1985.

Bastian AJ, Martin TA, Keating JG, and Thach WT. Cerebellar ataxia: abnormal control of interaction torques across multiple joints. *J Neurophysiol* 76: 492–509, 1996.

Bastian AJ, Zackowski KM, and Thach WT. Cerebellar ataxia: torque deficiency of torque mismatch between joints? *J Neurophysiol* 83: 3019–3030, 2000.

Beer RF, Dewald JPA, and Rymer WZ. Deficits in the coordination of multijoint arm movements in patients with hemiparesis: evidence for disturbed control of limb dynamics. *Exp Brain Res* 131: 305–319, 2000.

Bernstein NA. *The Co-ordination and Regulation of Movements.* Oxford, UK: Pergamon, 1967.

Bortolami SB, Pigeon P, Lackner JR, and DiZio P. Self-generated Coriolis forces on the arm during natural turning and reaching movements. *Soc Neurosci Abstr* 25: 1912, 1999.

Buneo CA, Jarvis MR, Batista AP, and Andersen RA. Direct visuomotor transformations for reaching. *Nature* 416: 632–636, 2002.

Caminiti R, Johnson PB, Galli C, Ferraina S, and Burnod Y. Making arm movements within different parts of space: the premotor and motor cortical representation of a coordinate system for reaching to visual targets. *J Neurosci* 11: 1182–1197, 1991.

Caminiti R, Johnson PB, and Urbano A. Making arm movements within different parts of space: dynamic aspects in the primate motor cortex. *J Neurosci* 10: 2039–2058, 1990.

Cockell DL, Carnahan H, and McFadyen BJ. A preliminary analysis of the coordination of reaching, grasping, and walking. *Percept Mot Skills* 81: 515–519, 1995.

Dean J and Brüwer M. Control of human arm movements in two dimensions: paths and joint control in avoiding simple linear obstacles. *Exp Brain Res* 97: 497–514, 1994.

Flanagan JR and Rao AK. Trajectory adaptation to a nonlinear visuomotor transformation: evidence of motion planning in visually perceived space. *J Neurophysiol* 74: 2174–2178, 1995.

Flanders M, Daghestani L, and Berthoz A. Reaching beyond reach. *Exp Brain Res* 126: 19–30, 1999.

Flash T and Hogan N. The coordination of arm movements: an experimentally confirmed mathematical model. *J Neurosci* 5: 1688–1703, 1985.

Georgopoulos AP, Kalaska JF, Caminiti R, and Massey JT. On the relations between the direction of two-dimensional arm movements and cell discharge in primate motor cortex. *J Neurosci* 2: 1527–1537, 1982.

Georgopoulos AP, Kettner RE, and Schwartz AB. Primate motor cortex and free arm movements to visual targets in three-dimensional space. II. Coding of the direction of movement by a neuronal population. *J Neurosci* 8: 2928–2937, 1988.

Gordon J, Ghilardi MF, and Ghez C. Accuracy of planar reaching movements. I. Independence of direction and extent variability. *Exp Brain Res* 99: 97–111, 1994.

Gower JC. Generalized Procrustes analysis. *Psychometrika* 40: 33–51, 1975.

Haggard P, Hutchinson K, and Stein J. Patterns of coordinated multi-joint movement. *Exp Brain Res* 107: 254–266, 1995.

Haggard P and Richardson J. Spatial patterns in the control of human arm movement. *J Exp Psychol Hum Percept Perform* 22: 42–62, 1996.

Hollerbach JM and Flash T. Dynamic interactions between limb segments during planar arm movement. *Biol Cybern* 44: 67–77, 1982.

Hong D, Corcos DM, and Gottlieb GL. Task dependent patterns of muscle activation at the shoulder and elbow for unconstrained arm movements. *J Neurophysiol* 71: 1261–1265, 1994.

Johnson RA and Wichern DW. *Applied Multivariate Statistical Analysis.* Englewood Cliffs, NJ: Prentice-Hall, 1992.

Kakei S, Hoffman DS, and Strick PL. Muscle and movement representations in the primary motor cortex. *Science* 285: 2126–2139, 1999.

Kakei S, Hoffman DS, and Strick PL. Direction of action is represented in the ventral premotor cortex. *Nat Neurosci* 4: 1020–1025, 2001.

Kalaska JF, Cohen DAD, Hyde ML, and Prud'Homme M. A comparison of movement direction-related versus load direction-related activity in primate motor cortex, using a two-dimensional reaching task. *J Neurosci* 9: 2080–2102, 1989.

Kalaska JF, Scott SH, Cisek P, and Sergio LE. Cortical control of reaching movements. *Curr Opin Neurobiol* 7: 849–859, 1997.

Lackner JR and DiZio P. Rapid adaptation to Coriolis force perturbations of arm trajectory. *J Neurophysiol* 72: 299–313, 1994.

Lacquaniti F, Soechting JF, and Terzuolo SA. Path constraints on point-to-point arm movements in three-dimensional space. *Neuroscience* 17: 313–324, 1986.

Lashley KS. Basic neural mechanisms in behavior. *Psychol Rev* 37: 1–24, 1930.

Ma S and Feldman AG. Two functionally different synergies during arm reaching movements involving the trunk. *J Neurophysiol* 73: 2120–2122, 1995.

Marteniuk RG, Ivens CJ, and Bertram CP. Evidence of motor equivalence in a pointing task involving locomotion. *Mot Control* 4: 165–184, 2000.

Morasso P. Spatial control of arm movements. *Exp Brain Res* 42: 223–227, 1981.

Morrison S and Newell KM. Inter- and intra-limb coordination in arm tremor. *Exp Brain Res* 110: 455–464, 1996.

Nishikawa KC, Murray ST, and Flanders M. Do arm postures vary with the speed of reaching? *J Neurophysiol* 81: 2582–2586, 1999.

Pigeon P, Yahia LH, Mitnitski AB, and Feldman AG. Superposition of independent units of coordination during pointing movements involving the trunk with and without visual feedback. *Exp Brain Res* 131: 336–349, 2000.

Pigeon P, Bortolami SB, DiZio P, and Lackner JR. Coordinated turn-and-reach movements. I. Anticipatory compensation for self-generated Coriolis and interaction torques. *J Neurophysiol* 89: 276–289, 2003.

Pozzo T, McIntyre J, Cheron G, andPapaxanthis C. Hand trajectory formation during whole body reaching movements in man. *Neurosci Lett* 240: 159–162, 1998.

Pozzo T, Stapley PJ, and Papaxanthis C. Coordination between equilibrium and hand trajectories during whole body pointing movements. *Exp Brain Res* 144: 343–350, 2002.

Robertson EM and Miall RC. Multi-joint limbs permit a flexible response to unpredictable events. *Exp Brain Res* 117: 148–152, 1997.

Rosenbaum DA, Engelbrecht SE, Bushe MM, and Loukopoulos LD. Knowledge model for selecting and producing reaching movements. *J Mot Behav* 25: 217–227, 1993.

Sainburg RL, Ghilardi MF, Poizner H, and Ghez C. Control of limb dynamics in normal subjects and patients without proprioception. *J Neurophysiol* 73: 820–835, 1995.

Schwartz AB. Motor cortical activity during drawing movements: single-unit activity during sinusoid tracing. *J Neurophysiol* 68: 528–541, 1992.

Schwartz AB. Motor cortical activity during drawing movements: population representation during sinusoid tracing. *J Neurophysiol* 70: 28–36, 1993.

Scott SH and Kalaska JF. Reaching movements with similar hand paths but different arm orientations. I. Activity of individual cells in motor cortex. *J Neurophysiol* 77: 826–852, 1997.

Scott SH, Sergio LE, and Kalaska JF. Reaching movements with similar hand paths but different arm orientations. II. Activity of individual cells in dorsal premotor cortex and parietal area 5. *J Neurophysiol* 78: 2413–2426, 1997.

Seidler RD, Alberts JL, and Stelmach GE. Multijoint movement control in Parkinson's disease. *Exp Brain Res* 140: 335–344, 2001.

Shadmehr R and Mussa-Ivaldi FA. Adaptive representation of dynamics during learning of a motor task. *J Neurosci* 14: 3208–3224, 1994.

Soechting JF, Buneo CA, Herrmann U, and Flanders M. Moving effortlessly in three dimensions: does Donders' law apply to arm movement? *J Neurosci* 15: 6271–6280, 1995.

Soechting JF and Lacquaniti F. Invariant characteristics of a pointing movement in man. *J Neurosci* 1: 710–720, 1981.

Topka H, Konczak J, Schneider K, Boose A, and Dichgans J. Multijoint arm movements in cerebellar ataxia: abnormal control of movement dynamics. *Exp Brain Res* 119: 493–503, 1998.

Wang J and Stelmach GE. Coordination among the body segments during reach-to-grasp action involving the trunk. *Exp Brain Res* 123: 346–350, 1998.

Wolpert DM, Ghahramani Z, and Jordan MI. Are arm trajectories planned in kinematic or dynamic coordinates? An adaptation study. *Exp Brain Res* 103: 460–470, 1995.

Zhang X and Chaffin DB. The effects of speed variation on joint kinematics during multisegment reaching movements. *Hum Mov Sci* 18: 741–757, 1999.